The Active Site Base Controls Cofactor Reactivity in *Escherichia coli* Amine Oxidase: X-ray Crystallographic Studies with Mutational Variants[†,‡]

Jeremy M. Murray, Colin G. Saysell, Carrie M. Wilmot, Winston S. Tambyrajah, Joachim Jaeger, Peter F. Knowles, Simon E. V. Phillips, and Michael J. McPherson*

School of Biochemistry and Molecular Biology, University of Leeds, Leeds LS2 9JT, United Kingdom

Received January 7, 1999; Revised Manuscript Received April 9, 1999

ABSTRACT: Amine oxidases utilize a proton abstraction mechanism following binding of the amine substrate to the C5 position of the cofactor, the quinone form of trihydroxyphenylalanine (TPQ). Previous work [Wilmot, C. M., et al. (1997) *Biochemistry 36*, 1608−1620] has shown that Asp383 in *Escherichia coli* amine oxidase (ECAO) is the catalytic base which performs the key step of proton abstraction. This paper explores in more depth this and other roles of Asp383. The crystal structures of three mutational variants are presented together with their catalytic properties, visible spectra, and binding properties for a substrate-like inhibitor, 2-hydrazinopyridine (2-HP), in comparison to those of the wild type enzyme. In wild type ECAO, the TPQ is located in a wedge-shaped pocket which allows more freedom of movement at the substrate binding position (C5) than for TPQ ring carbons C1−C4. A role of Asp383, whose carboxylate is located close to O5, is to stabilize the TPQ in its major conformation in the pocket. Replacement of Asp383 with the isostructural, but chemically distinct, Asn383 does not affect the location or dynamics of the TPQ cofactor significantly, but eliminates catalytic activity and drastically reduces the affinity for 2-HP. Removal of the side chain carboxyl moiety, as in Ala383, additionally allows the TPQ the greater conformational flexibility to coordinate to the copper, which demonstrates that Asp383 helps maintain the active site structure by preventing TPQ from migrating to the copper. Glu383 has a greatly decreased catalytic activity, as well as a decreased affinity for 2-HP relative to that of wild type ECAO. The electron density reveals that the longer side chain of Glu prevents the pivotal motion of the TPQ by hindering its movement within the wedge-shaped active site pocket. The results show that Asp383 performs multiple roles in the catalytic mechanism of ECAO, not only in acting as the active site base at different stages of the catalytic cycle but also in regulating the mobility of the TPQ that is essential to catalysis.

Copper-containing amine oxidases (EC 1.4.3.4) are widely distributed among prokaryotic and eukaryotic organisms where they catalyze the two-electron oxidative deamination of amines according to the reaction

$$RCH_2NH_3^+ + O_2 + H_2O \rightarrow RCHO + NH_4^+ + H_2O_2$$

Catalysis appears to involve a ping-pong bi ter mechanism with reductive and oxidative half-cycles (*1*) (Figure 1).

In prokaryotic organisms, these enzymes are involved in nutrient catabolism, but in higher organisms, their roles are more complex. In mammals and plants, there are tissue-specific forms involved in cell signaling, growth and development, and cell death potentially (*2*−*4*). Medical interest in amine oxidases is increasing because of reports which conclude that they mediate interactions between lymphocytes and endothelial cells (*5*), the formation of vas-

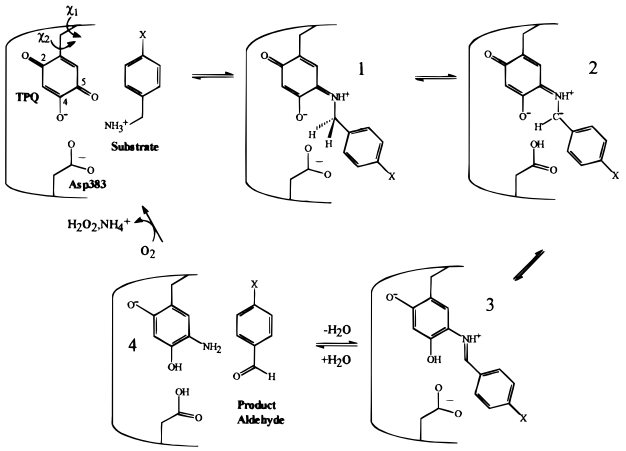

FIGURE 1: Pathway for the catalytic cycle of *E. coli* copper amine oxidase. The TPQ numbering scheme and the definition of torsion angles, χ_1 and χ_2, are shown, along with the active site base, Asp383, and the substrate as a substituted phenylmethylamine. The substrate is first deprotonated and then forms the substrate Schiff base C5 (step 1). Asp383 then abstracts a hydrogen from the methylene group (step 2), and a rearrangement leads to the product Schiff base (step 3). Hydrolysis releases the product aldehyde, leaving the enzyme in a reduced state (step 4). Reoxidation of the enzyme by molecular oxygen releases ammonia and hydrogen peroxide, and regenerates the active form.

[†] This work was supported by grants from the UK Biotechnology and Biological Sciences Research Council (BBSRC) and the Engineering and Physical Sciences Research Council to P.F.K., S.E.V.P., and M.J.M. and the Howard Hughes Medical Institute for an International Research Scholar award to S.E.V.P. A BBSRC Special Studentship supported J.M.M.

[‡] File Names for Brookhaven Protein Structure Data Bank entries: wild type, 1JEZ; D383E variant, 1QAF; D383A variant, 1QAK; and D383N variant, 1QAL.

* To whom correspondence should be addressed: School of Biochemistry and Molecular Biology, University of Leeds, Leeds LS2 9JT, U.K. Telephone: +44 113 2332595. Fax: +44 113 233 3144. E-mail: m.j.mcpherson@leeds.ac.uk.

10.1021/bi9900469 CCC: $18.00
Published on Web 06/09/1999

cular plaques implicated in congestive heart failure (*6*), and vascular damage observed in late-diabetic complications.

The copper amine oxidases have been the subject of biochemical, spectroscopic, and kinetic studies for many years (*7*, *8*). These studies have shown that amine oxidases contain an organic cofactor 2,4,5-trihydroxyphenylalanine quinone (TPQ,[1] Figure 1) in addition to copper (*9*). The formation of the TPQ cofactor by the post-translational modification of a tyrosine residue within the active site consensus sequence T-X-X-N-Y-D/E involves self-processing events requiring both copper and molecular oxygen (*10*−*12*).

The determination of the structure of *Escherichia coli* amine oxidase at 2 Å resolution (ECAO) (*13*) and subsequently of amine oxidases from pea seedling (PSAO) (*14*), *Arthrobacter globiformis* (AGAO) (*15*), and *Hansenula polymorpha* (HPAO) (*16*) have provided structural frameworks for investigation of the molecular basis for catalysis in these enzymes. The copper amine oxidases are homodimers with a subunit size of approximately 70−95 kDa depending on the source. The enzymes are predominantly β-structure with a large catalytic domain and two or three smaller peripheral domains.

It is an intriguing feature of the report by Parsons et al. (*13*) that there were two alternate locations for the TPQ cofactor. In inactive crystals grown from ammonium sulfate, TPQ was coordinated to the copper via O4, while it was positioned away from the copper in the active crystals grown from citrate, with O4 hydrogen bonded to Oη of the conserved tyrosine 369. This implied that the position of the TPQ was important in activity (Figure 2). There are also differences in the orientation and mobility of the TPQ ring in the amine oxidase structures from the different sources, suggesting that conformational changes in the TPQ could be important in amine oxidase function. Rotation of the TPQ ring during its self-processing from tyrosine has also been proposed (*15*, *17*, *18*). In the active form, the copper is coordinated by three histidines and two water molecules in a square pyramidal arrangement. In the inactive form, the axial water is replaced by O4 of TPQ and the equatorial water is lost, leading to tetrahedral geometry.

The reductive half-cycle of the catalytic mechanism can be considered in the context of the structure of the active site (Figure 1). The substrate amine is initially deprotonated by an active site base (*1*, *19*) that facilitates formation of a substrate Schiff base at the C5 position of TPQ (Figure 1, step 0 to 1). The protonated base then acts as a general acid in the elimination of TPQ O5 as water from the carbinolamine intermediate. As a consequence, it is able to abstract the C−H proton from the methylene group of the substrate Schiff base to give the product Schiff base (Figure 1, step 1 to 2). The product Schiff base is then hydrolyzed to give the aminoquinol form of the TPQ, and product aldehyde is released (Figure 1, step 3 to 4). In the oxidative half-cycle, molecular oxygen binds to the enzyme and regenerates the active form with evolution of hydrogen peroxide and ammonia. Wilmot et al. (*20*) provided strong evidence that Asp383 acts as the active site base in *E. coli* amine oxidase

[1] Abbreviations: TPQ, 2,4,5-trihydroxyphenylalaninequinone; ECAO, *E. coli* amine oxidase; PSAO, pea seedling amine oxidase; AGAO, *A. globiformis* amine oxidase; HPAO, *H. polymorpha* amine oxidase; PPAO, pig plasma amine oxidase; 2-HP, 2-hydrazinopyridine.

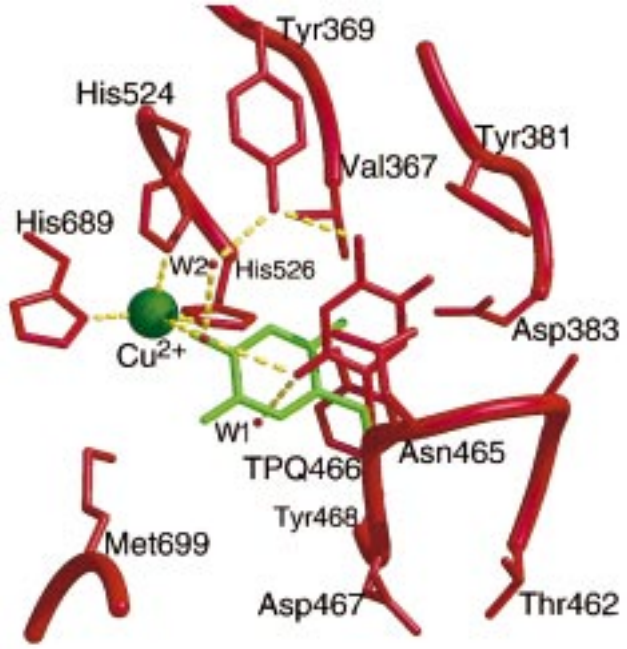

FIGURE 2: Active site of *E. coli* copper amine oxidase. The new high-resolution wild type structure is shown in red with residues numbered and the TPQ (residue 466) in the normal "off-copper" conformation. The copper is shown as a green sphere, and water molecules (W) mentioned in the text are also labeled. The position of the TPQ in the inactive form crystallized from ammonium sulfate is shown in green and represents the "on-copper" conformation (*13*).

by (i) the demonstration that site-directed mutational variants at Asp383, with the exception of Glu383, had no activity even though they were shown to contain the TPQ cofactor and (ii) the determination of the structure of the complex between the enzyme and the inhibitor 2-hydrazinopyridine that showed the inhibitor was bound at the 5 position of the TPQ ring and lay close to Asp383. The importance of Tyr369, a conserved residue in the active site, in anchoring the position of the TPQ via a hydrogen bond to O4 was clearly evident in the structure of the complex.

This paper explores in more depth the roles of Asp383 in *E. coli* amine oxidase. The structures of three mutational variants (D383E, D383A, and D383N) are presented together with their visible spectra and binding properties with respect to the inhibitor 2-hydrazinopyridine. The data provide strong evidence that in the native enzyme, Asp383 performs multiple roles that include stabilizing the TPQ in an "off-copper" conformation, assisting substrate binding to TPQ and abstracting the C−H proton from the substrate.

EXPERIMENTAL PROCEDURES

Mutagenesis, Expression, and Protein Purification. The *ecao* gene was mutated using the PCR megaprimer method (*21*). The following oligonucleotides were used to introduce point mutations

5'-AGTCACC**GCT** ***AGC*** CAGATACGCTTTAAAG-3' (D383A);

5'-AGTCACCAGA ***C*** TC **G** AGATACGCTTTAAAG-3' (D383E) and;

5'-CACCAGA ***ATT*** CAGATACGCTTTAAAGTACC-3' (D383N)

The mutations to alter the Asp383 codon are shown in bold

Table 1: Data Collection and Processing Statistics for *E. coli* Copper Amine Oxidase Wild Type (WT), D383E, D383A, and D383N[a]

	WT[b]	D383E[c]	D383A[d]	D383N[e]
λ (Å)	0.99	1.488	0.87	0.9
d_{min} (Å)	2.04	2.2	2.0	2.2
no. of unique reflections	105826	84390	109772	87702
multiplicity	3.2	2.9	2.8	2.9
completeness (%)	93.3	91.6	91.4	93.7
$I/\sigma I$ (final shell)	7.9 (3.4)	8.3 (3.2)	7.1 (3.9)	6.6 (2.7)
R_{symm} (%)(final shell)	5.8 (19.0)	6.6 (20.4)	6.7 (16.4)	7.2 (22.3)

[a] All X-ray diffraction data were collected at 100 K on a MAR 300 mm image plate with proteins that crystallized in orthorhombic space group $P2_12_12_1$ with similar unit cell dimensions (a = 135.0 Å, b =167.0 Å, and c = 78.0 Å) and one noncrystallographic ECAO dimer per asymmetric unit. [b] Beamline ID2, ESRF. [c] Beamline 7.2, Daresbury SRS. [d] Beamline 9.6, Daresbury SRS. [e] Beamline 9.5, Daresbury SRS.

italics, and mutations for introducing *Nhe*I, *Xho*I, and *Eco*RI restriction sites, respectively, are bold and underlined. The mutated codon is boxed, and the sequence of the mutated gene was confirmed by DNA sequence analysis of both strands of the mutant genes using dideoxynucleotide sequencing with fluorescent terminators and an ABI 373 instrument (Perkin-Elmer). The *E. coli* overexpression system used for the production of the wild type and mutational variants of ECAO was based on the vector pKK233-3 (Amersham-Pharmacia). Cells were grown in 2TY growth medium (*22*) containing 55 μM $CuSO_4$, 50 mg/mL ampicillin, and 25 mg/mL carbenicillin to an OD_{600} of 0.6−0.7. Protein expression was induced by adding isopropyl β-D-thiogalactopyranoside (IPTG; Melford Laboratories Ltd.) to a final concentration of 3.5 mM and allowing growth to continue for a further 4 h. All proteins were purified using previously reported protocols (*13*, *20*).

X-ray Crystallographic Data Collection. Crystals of wild type and mutant ECAO were grown from 1.3 M sodium citrate and 100 mM HEPES buffer at pH 7.1 using the sitting drop vapor diffusion method. They were transferred briefly to a cryoprotectant solution containing 20% glycerol before flash-cooling to 100 K in a cold nitrogen gas stream. Diffraction data were collected at 100 K using the ESRF (European Synchrotron Radiation Source) or Daresbury SRS (Synchrotron Radiation Source) with 300 mm MAR imaging plate detectors. The diffraction patterns were markedly anisotropic, with diffraction extending further in the *a*- and *b*-axis directions than along the *c*-axis, as noted previously for frozen ECAO crystals (*20*). The reflections were integrated using MOSFLM (*23*), and all subsequent merging and scaling was performed using programs from the CCP4 suite (*24*). Details of crystal parameters, data collection, and processing statistics are shown in Table 1.

Structure Determination. The initial model for the wild type structure was generated from the previously determined 2.4 Å room-temperature structure (*13*) by replacing the TPQ (residue 466) in each subunit with an alanine residue and removing water molecules from the vicinity of the active site. Starting models for the three mutant proteins were generated in a similar way but with Asp383 also replaced with alanine in each case. Because of the slight shrinkage in the unit cells (2−3% mainly in *c*) relative to the room-temperature structure, each model was first subjected to 60 cycles of rigid body refinement using the program CNS (*25*). The resulting models were used to calculate σ_A-weighted $2F_o - F_c$, $F_o - F_c$, and, for the mutants, $F_{oWT} - F_{omutant}$ electron density maps (*26*). The computer graphics program O (*27*) was used to build the missing side chains for residues 383 and 466 (TPQ) where possible, as well as making minor adjustments elsewhere in the structure where indicated by the maps. Models were subjected to rounds of refinement and rebuilding, using maximum likelihood refinement (*28*), where each round consisted of 100 cycles of tightly restrained positional refinement, with anisotropic overall *B*-factor refinement, and 50 cycles of individual temperature factor refinement. In CNS refinements, the copper−ligand distances were treated as nonbonding interactions where parameters for the copper were determined from small molecule crystal structures deposited in the Cambridge Crystallographic Database. These parameters lead to a shallow restraint energy minimum at 2.12 Å for Cu−N distances. A bulk solvent correction was applied once per round to all data from 50.0 Å to the diffraction limit. After the first pass, the individual atomic *B*-factors were reset to the average values calculated over all atoms, and then further subjected to 20 cycles of *B*-factor refinement. In the final stages of refinement, the program REFMAC (*24*) was used, with all data from 20 Å to the diffraction limits, taking advantage of its treatment of anisotropic diffraction data, and removing the restraint on Cu−N distances completely.

Mass Spectroscopic Analysis of Metal Content. Samples of wild type ECAO and of the D383A mutational variant were analyzed by inductively coupled plasma mass spectrometry (ICP-MS) using a Platform ICP instrument (Micromass UK Ltd., Manchester, U.K.). The samples were analyzed in aqueous solution, monitoring for four elements: calcium, iron, zinc, and copper. A standard solution was prepared in the same solvent and analyzed under identical conditions so that an estimate of the quantities of these four elements could be made. The semiquantitative data obtained are expected to have a 10−15% error.

Enzyme Preparations for Solution Studies. The enzyme concentration, typically in the range of $1.0-6.0 \times 10^{-6}$ M, was determined from absorbance at 280 nm using an extinction coefficient of 2.1×10^5 M^{-1} cm^{-1} (*29*). The enzyme was dialyzed against 20 mM phosphate buffer (pH 7.0) at 4 °C and centrifuged prior to use.

Optical Spectra Studies. All UV−vis spectral studies were performed on a Shimadzu UV-2401PC spectrophotometer at 25.0 °C. Enzyme activity was measured as previously described using a coupled assay with β-phenylethylamine as the substrate (*13*).

Rapid Reaction Spectrophotometric Studies of Inhibitor Binding Kinetics. The reactions were monitored using an Applied Photophysics SX-17MV stopped-flow rapid reaction spectrophotometer at a fixed wavelength corresponding to the λ_{max} of the adduct as determined from the titration results.

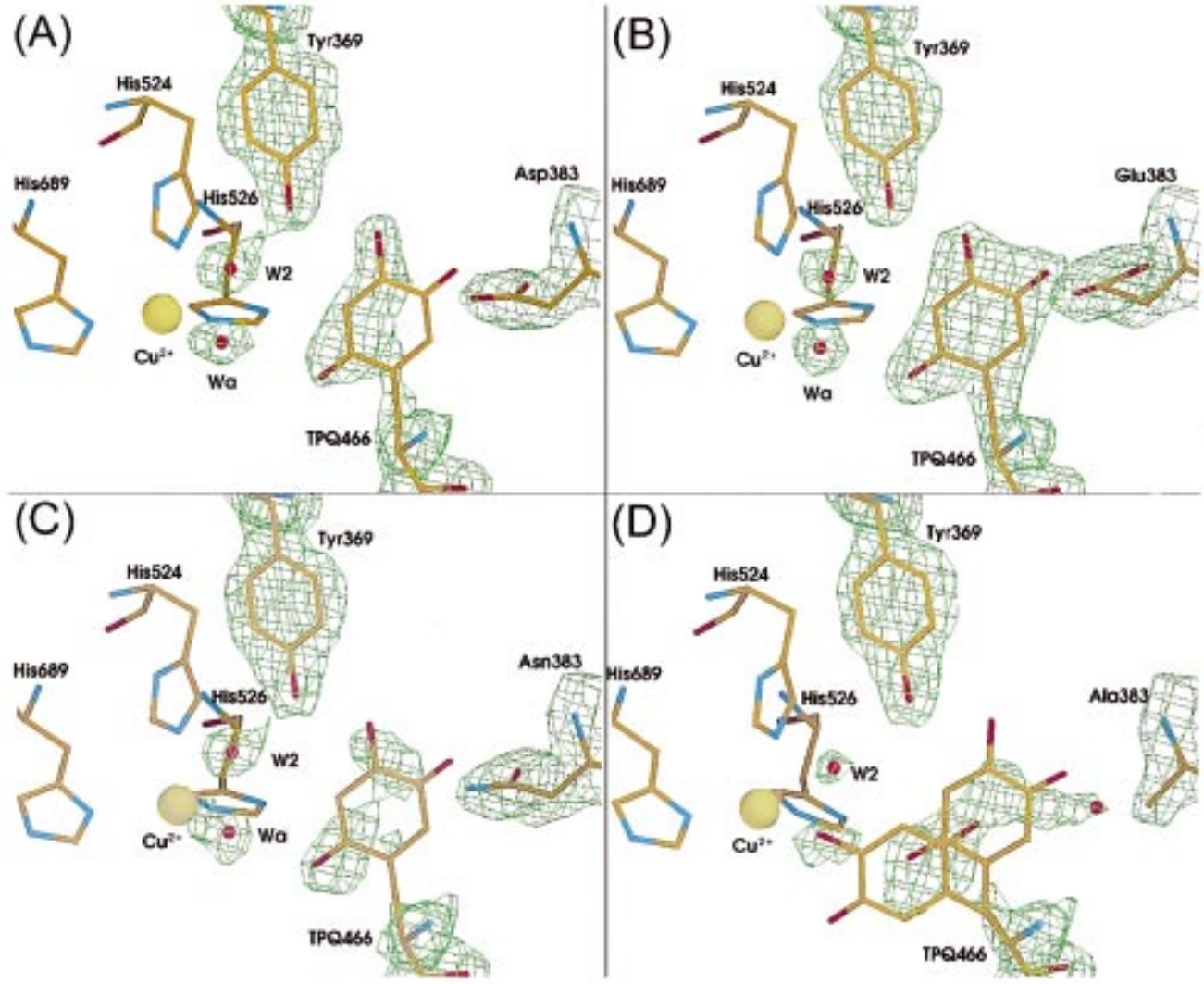

FIGURE 3: Electron density maps of the TPQ region of the *E. coli* copper amine oxidase wild type (A) and the (B) D383E, (C) D383N, and (D) D383A variants contoured to 1.6σ. The conformational rigidity or flexibility of the TPQ is apparent with well-defined density in D383E (B), reasonably defined density for C2−C4 in the wild type (A) and D383N (C), and less well-defined density for D383A (D) indicative of both on- and off-copper conformations.

For D383N and D383A, where λ_{max} was not known from the titration studies, it was determined by adding a 100-fold excess of 2-HP to a sample and recording the visible spectrum. Enzyme, typically 1.5−8.0 μM, was reacted with 2-HP present in a 10−3000-fold excess to ensure pseudo-first-order reaction conditions. It was found that increasing the 2-HP concentration above 5.0 mM (corresponding to a 3000-fold excess) affected the pH of the reaction mixture. Absorbance versus time traces were fitted using the Applied Photophysics SX-17MV software. The average of five absorbance versus time traces was taken to obtain the mean pseudo-first-order rate constant (k_{obs}) at each inhibitor concentration.

RESULTS

Wild Type ECAO Crystal Structure. Initial rigid body refinement of the wild type starting model, generated from the previous 2.4 Å room-temperature structure (*13*), reduced the *R*-factor from 38.7 to 24.9% at 50−4 Å. Maps calculated at this point clearly showed the positions of Asp383 in both subunits (A and B) of the noncrystallographic dimer that constitutes the asymmetric unit, but density for the TPQ was weak and poorly connected. The side chains for Asp383, and several well-defined water molecules, were added to the model, together with minor adjustments to several other side chains, followed by successive rounds of refinement and rebuilding. The electron density for TPQ was improved by this procedure but, although better defined than in the original room-temperature structure, showed clear signs of disorder. A major conformation was apparent, in both independent subunits, where O2 is directed toward, but not coordinated to, the copper and O5 faces Asp383. Further refinement showed this model to be a reasonable interpretation of the diffraction data, but the final refined maps demonstrate that the TPQ is poorly ordered and is highly mobile and/or subject to static disorder (Figure 3). Residues 1A−6A, 725A−727A, 1B−5B, and 726B and 727B showed no electron density and so were omitted from the model. No residues fall in the disallowed region of the Ramachandran plot as defined by PROCHECK (*30*). The refinement finally converged to an *R*-factor of 18.5% (R_{free} = 23.7%) for all data from 20 to 2.04 Å. Full refinement statistics are shown in Table 2.

The major orientation of TPQ corresponds to that found for the inhibitor complex, where 2-HP is covalently linked

Table 2: Crystallographic Refinement and Final Model Statistics

	WT ECAO	D383E	D383A	D383N
resolution range (Å)	20−2.04	20−2.2	20−2.0	20−2.2
no. of reflections in working set	98924	79295	105194	82486
no. of reflections in free set	3493	2781	3735	2901
no. of non-hydrogen atoms				
no. of amino acid residues	1449	1447	1448	1450
no. of protein atoms	11366	11356	11345	11368
no. of solvent molecules	1568	1406	1487	1546
no. of Cu^{2+} ions	2	2	2	2
no. of Ca^{2+} ions	4	4	4	4
R_{work} (%)	18.5	17.6	18.5	19.2
R_{free} (%)	23.7	24.4	24.0	24.9
B-factor				
protein atoms in the main chain/side chain (Å^2)	31.9/31.9	31.8/32.7	28.0/28.8	29.7/29.4
water molecules (Å^2)	44.7	40.9	37.6	40.9
rmsd from ideal geometry				
bonds (Å)	0.012	0.012	0.010	0.012
angles (deg)	2.9	3.6	3.1	3.0
Ramachandran plot				
energetically favored regions (%)	89.4	88.8	89.0	88.3
additionally allowed regions (%)	9.8	10.7	10.3	11.1
generously allowed regions (%)	0.7	0.5	0.6	0.6
disallowed regions (%)	0.0	0.1	0.1	0.0
rms distance of Cα atoms of variants onto WT (Å)				
A subunit		0.15	0.21	0.17
B subunit		0.17	0.21	0.21

to C5 (*20*) and is, presumably, a productive conformation for substrate binding. The level of disorder suggests, however, that the ring could probably flip about χ_2 (Figure 1) such that O5 could face the copper, and the more disordered room-temperature structure shows evidence of this as a major conformation. The electron density for the TPQ is much stronger for O2, O4, and the ring carbons from C1 to C4 but weakens for O5, C5, and C6 on the other side of the ring (Figure 3). If the contour level is greatly reduced, the electron density covers the entire TPQ ring and becomes continuous with that for Asp383. Inspection of the van der Waals surfaces of the residues surrounding TPQ shows that it lies in a wedge-shaped pocket (Figure 4). One face of TPQ lies against the amide group of the conserved Asn465, while the side chain of Val367 forms the other side of the pocket. These two surfaces are not parallel, however, and make close contacts with the edge of the TPQ along the C2−C4 side, but open out toward the other edge of the ring leaving it more freedom of movement perpendicular to the plane at O5, C5, and C6. The carboxylate of Asp383 lies near O5, positioned to stabilize the TPQ in its major conformation where it lies against the Asn465 surface of the pocket. Very small movements in Asp383 would be sufficient to allow TPQ to pivot to the other side of the pocket, leading to weaker electron density along one edge. This TPQ motion, where the C5−C6 edge of the ring moves more than the other edge, is a consequence of the shape of the pocket and can readily be accommodated by rotation about χ_2 accompanied by smaller rotations about χ_1 and small movements in the main chain. The refined temperature factors for TPQ ring atoms reflect this, rising to >50 Å^2 despite restraints, but are not sufficiently reliable at this resolution to allow a quantitative description. These observations could arise from thermal motion or static disorder and appear to represent a continuum of conformations within the pocket that cannot be reliably refined as multiple discrete conformations. In the A subunit, the major TPQ conformation has a contact of 3.1 Å from O5 to Oδ1 of Asp383 that could be either a van der Waals interaction or a hydrogen bond, implying ionization or protonation of the carboxylate, respectively. The disorder of the TPQ, however, precludes a firm assignment. In the B subunit, the corresponding distance is too long for a hydrogen bond and there is weak density that might indicate an intervening water molecule. Occasional minor differences between the A and B subunits will be described only where they are significant; otherwise, the parameters reported refer to the A subunit. On the basis of equivalent assignments made by Farnum et al. (*19*) on bovine serum amine oxidase, we assign the pK_a of 6.2 to Asp383 in ECAO on the basis of the pH dependence of k_{cat}/K_m (*20*). Therefore, Asp383 is likely to be almost fully ionized at the pH of 7.0 used in all the studies presented here. Previously, we erroneously assigned a p*K* of 8 to Asp383 (*20*) and are grateful to K. Tanizawa for pointing out this error. Evidence for varying degrees of TPQ mobility is also apparent in the structures of amine oxidases from other species (*14*−*16*). By contrast, the ammonium sulfate-inactivated form of ECAO and one data set for holo-AGAO have a well-ordered TPQ coordinated to the copper (*13*−*15*).

Elsewhere, the structure is essentially identical to that determined at room temperature with a few minor exceptions, the most notable being in the details of copper coordination. In the room-temperature structure (*13*), the copper has square pyramidal coordination, with three histidines (524, 526, and 689) and a water molecule as equatorial ligands, and an axial water ligand (Figure 2). In these studies of crystals at 100 K, the equatorial water is clearly missing in both subunits of the wild type structure, while the histidines are unchanged. The equatorial water is present, however, in the structure of the 2-HP inhibitor complex at 100 K (*20*), but with a long coordination distance to the copper (3.0 Å as opposed to

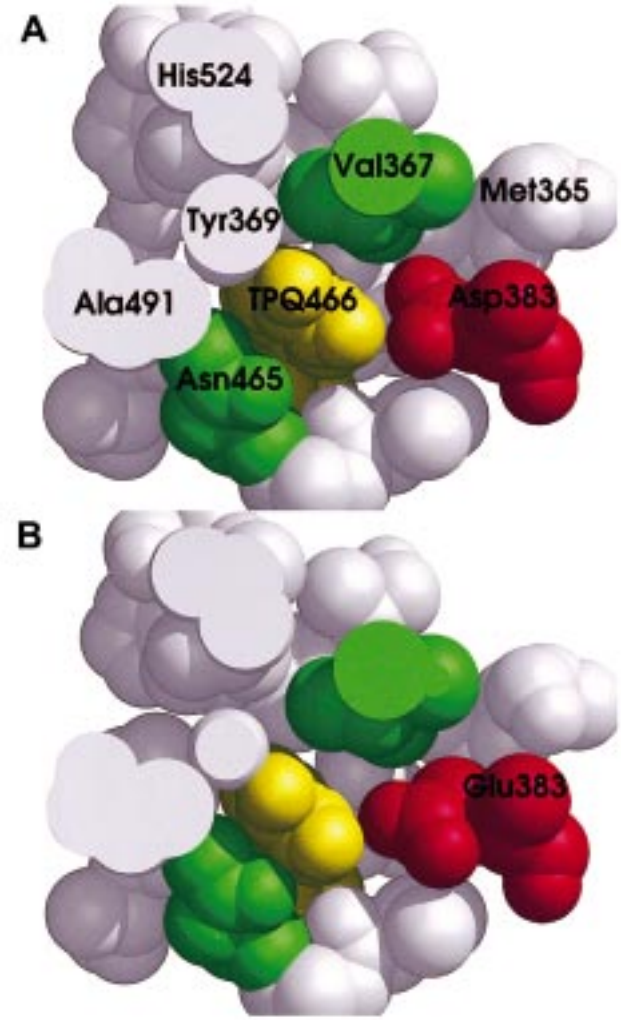

FIGURE 4: Space-filling representation of the region surrounding TPQ (yellow) in the off-copper conformation in (A) the wild type and (B) D383E. Residues are labeled, and those forming the wedge-shaped pocket are shown in green. Asp383 and Glu383 are shown in red, and the intrusion of the latter into the wedge-shaped pocket limits conformational flexibility of the TPQ.

2.0 Å in the wild type at room temperature). In the HPAO structure (*16*), this water is present in only five of the six subunits of the three independent dimers and, where present, is variable in position, lying approximately 3 Å from the copper. It therefore appears to be labile and sensitive to small changes in environment or conditions. The nearby side chain of Met699 is also not fully ordered in ECAO and has been built in its predominant orientation. The remaining water structure in the active site is little changed, with a particularly well-ordered molecule (W2) forming a hydrogen-bonded bridge between Oη of Tyr369 and the axial water on the copper (Figure 5) as also observed in the HPAO structure (*16*).

Apart from the copper, the ECAO structure contains two further metal ions per subunit that are distant from the active site and whose function is unknown, although they may simply have a structural role. Both ions were proposed to be Ca^{2+} by Parsons et al. (*13*) on the basis of the coordination geometry and crystallographic refinement. This is supported by the mass spectrometry results reported below.

D383A Structure. Structure solution for D383A followed the same procedure as for the wild type, with rigid body refinement reducing the *R*-factor to 29.1%. Maps showed the expected lack of density beyond Cβ of Ala383, and the density for the TPQ suggested greater disorder than for the wild type, with evidence of two conformations. In one conformation, O4 is coordinated to the copper and differs from the active wild type structure but is identical to that originally found in the inactivated form (*13*). In this conformation, the axial water has been displaced by TPQ and the equatorial water remains absent, leading to tetrahedral copper coordination. Since the two conformations are resolved from one another, the disordered TPQ could be discretely refined with a 75% contribution of "on-copper" ("25% off-copper") giving similar temperature factors (50−60 Å^2) for the TPQ ring atoms. The conclusion is that both forms are present as a statistically disordered mixture, with the majority contribution from the "on-copper" conformation, but the treatment is only qualitative at this resolution. Elsewhere, the structure was little changed, and following rounds of rebuilding, refinement finally converged to an *R*-factor of 18.5% (R_{free} = 24.0%) for all data from 20 to 2.0 Å with good geometry (Table 2).

D383N Structure. Rigid body refinement of D383N led to an *R*-factor of 20.5%, and maps showed the fully ordered side chain Asn383 in a position identical to that of Asp383 in the wild type (Figure 5). In fact, D383N exhibits very similar disorder in the TPQ density and is essentially isostructural with respect to the wild type, as demonstrated by the very low *R*-factor that was observed after initial rigid body refinement, with a very weak density peak suggesting partial occupancy for the equatorial water molecule coordinated to the copper. Rebuilding and refinement followed the same course, therefore, as for wild type, converging to a final *R*-factor of 19.2% (R_{free} = 24.9%) for all data from 20 to 2.2 Å with good geometry (Table 2).

D383E Structure. Following rigid body refinement (*R*-factor = 26.2%), maps showed clear electron density for the side chain of Glu383, in a position similar to that of Asp383, but also strong density corresponding to the TPQ. In both subunits, the TPQ is well-ordered and in an orientation similar to the major conformation in the wild type (Figure 5). Temperature factors for TPQ ring atoms lie in the range of 25−35 Å^2, similar to those of the surrounding side chains and much lower than those for TPQ in the wild type structure. The distances from TPQ O5 to Oϵ2 of Glu383 are 3.5 Å, in both the A and B subunits, a little too long for a hydrogen bond, leaving the protonation state of the carboxylate uncertain. The rest of the structure is very similar to the wild type and the other mutants, except for the orientation of the Tyr381 side chain. This tyrosine acts as a gate at the enzyme surface, closing off a channel leading from the exterior to the binding site for the amine substrate (*15*, *20*). In the wild type ECAO structure, it is well-defined but relatively mobile, while in the 2-HP inhibitor complex, it has been pushed out of the way by the 2-HP adduct and stands in an "open" position. It also has the open conformation in the D383E structure, leaving the active site more accessible to solvent. The equatorial water on the copper is also present in D383E, at a distance of 3.1 Å, but only in subunit B. Following rounds of rebuilding, refinement finally converged to an *R*-factor of 17.6% (R_{free} = 24.4%) for all data from 20 to 2.2 Å with good geometry (Table 2).

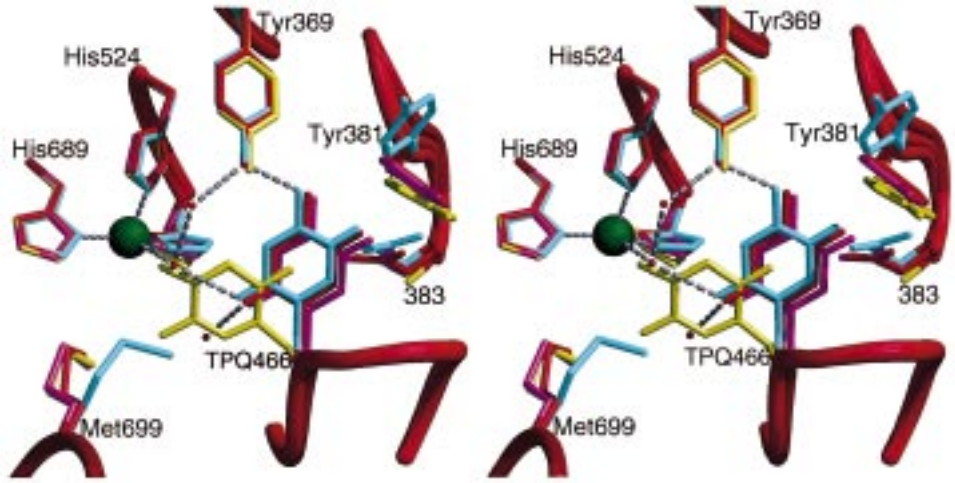

FIGURE 5: Stereoview of the superposition of the active sites of the wild type (red), D383N (violet), D383E (cyan), and D383A (yellow) from a perspective similar to that shown in Figure 2 in which relevant residues are labeled.

Comparison of the Structures. The overall structures of the three mutants are all closely similar, with rms deviations for Cα atoms of 0.21, 0.19, and 0.16 Å for D383A, -N, and -E, respectively, relative to the wild type structure. Changes are restricted to the vicinity of the active site, and a local superposition of the structures is shown in Figure 5. The most obvious, and striking, difference is the location of the TPQ ring, which adopts a similar off-copper conformation, albeit with varying degrees of order, in all but the D383A mutant. In D383A, there is a significant proportion of the on-copper conformation where O4 supplies the axial ligand to the copper, displacing the axial water molecule present in all the other structures. Two other small differences are present only in the D383A mutant: a small rotation of the ring of the copper ligand His526 and a slight shift of the "gate" Tyr381 toward the space vacated by the TPQ when in the on-copper conformation.

The D383N mutant appears to be identical to the wild type, even to the degree of disorder of the TPQ, but the apparently subtle mutation D383E has structural consequences. The extra methylene group in Glu383 causes its carboxylate to protrude a little further over the TPQ and restricts the freedom of the ring in pivoting toward Val367 by intruding into the wide end of the wedge-shaped pocket (Figure 4). This causes the TPQ to move away slightly, packing a little more closely on Asn465 and becoming well-ordered. The distance between the D383E carboxylate oxygens and TPQ O5 is maintained as slightly longer than a hydrogen bond, as in the wild type. Tyr381 has, however, swung away from its normal position where it closes the channel to the surface possibly because, had it remained in the wild type conformation, there would be an unfavorably close contact (<3 Å) to Glu383 Oε1. The new position corresponds to the open conformation observed in the 2-HP inhibitor complex (*20*). The other obvious change is the movement of Met699, but this side chain is poorly ordered and the significance of the change uncertain.

The water structure in the active site varies slightly between the different structures near the TPQ and position 383 side chain, but a very well-ordered water W2 (Figure 2) is always found hydrogen bonded between the conserved Tyr369 and the axial copper ligand (water or TPQ). This water is conserved in all known amine oxidase structures.

Metal Analysis by Mass Spectrometry. The metal analyses (in nanograms per milliliter) averaged over all isotopes of each metal were as follows: wild type ECAO, 3882 ± 781 Ca, 8 ± 1 Fe, 6120 ± 6 Cu, and 630 ± 44 Zn; and D383A, 2738 ± 529 Ca, 5 ± 7 Fe, 5591 ± 243 Cu, and 168 ± 14 Zn. These results lead to ratios for Ca/Cu of 0.97 and for Zn/Cu of 0.1 for wild type ECAO and ratios for Ca/Cu of 0.75 and for Zn/Cu of 0.03 for D383A. Accepting partial occupancy at the two metal ion sites observed per subunit remote from the active site, the Ca/Cu ratios on the two samples provide strong support for the proposal of ref *13* that electron density at these sites is due to calcium.

Enzyme Activity. The D383E variant yielded a K_m value of 2.5 ± 0.2 μM and a k_{cat} per dimer of 0.075 ± 0.001 s^{-1} compared to values for the wild type enzyme of 1.2 ± 0.07 μM and 118 ± 1.7 s^{-1}, respectively. Clearly, the major effect of the mutation is on turnover rather than on substrate binding. No activity could be measured for the D383A and D383N mutational variants under conditions where activity could be detected at a 10^7-fold dilution of the wild type enzyme.

Optical Absorption spectra. The visible spectra are shown in Figure 6. It can be seen that the spectral characteristics of the wild type (ε value of 3660 M^{-1} cm^{-1} at a λ_{max} of 480 nm) and D383E (ε value of 3460 M^{-1} cm^{-1} at a λ_{max} of 480 nm) are nearly indistinguishable. However, spectral changes are evident for D383A (ε of 3810 M^{-1} cm^{-1} at a λ_{max} of 444 nm) and D383N (ε of 3460 M^{-1} cm^{-1} at a λ_{max} of 450 nm). Consistent with this, solutions of the wild type and D383E were pink, while D383N was orange and D383A yellow.

Kinetics of 2-Hydrazinopyridine Binding. The results for the kinetics of inhibitor binding to the wild type and mutational variant forms of ECAO are shown in Figure 7. Saturation kinetics were observed for the wild type enzyme, while for the variants, saturation was not achieved, although there are indications of curvature toward it. Double-reciprocal plots of the data allow values for apparent $K_{binding}$ and the maximum pseudo-first-order rate constant ($k_{obs-max}$) to be determined (wild type) or extrapolated (variants) (Table 3).

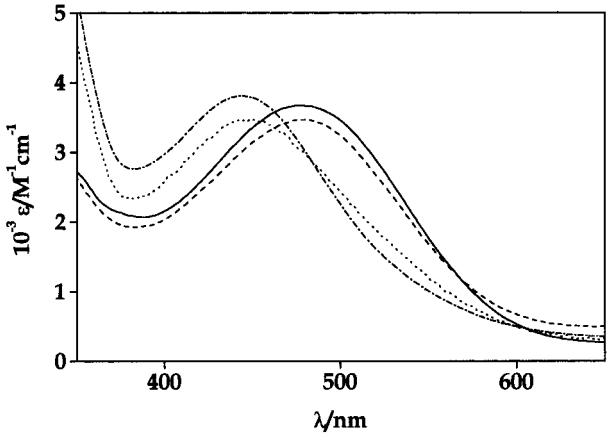

FIGURE 6: UV−visible spectra of wild type *E. coli* amine oxidase (—), D383E (- - -), D383N (•••), and D383A (-•-). All spectra were recorded at 25 °C in 100 mM Hepes buffer (pH 7.0) at an ionic strength of 0.1 M.

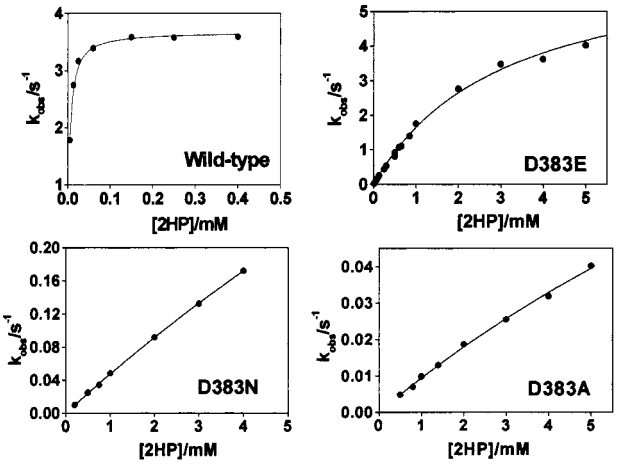

FIGURE 7: Dependence of pseudo-first-order rate constants on 2HP concentration for formation of the TPQ−2-HP adduct in wild type *E. coli* amine oxidase and three D383 catalytic base variants. All reactions were conducted at 25 °C in 100 mM Hepes buffer (pH 7.0) at an ionic strength of 0.1 M.

Table 3: Kinetics of 2-Hydrazinopyridine Binding to the ECAO Wild Type and Variants

enzyme form	apparent $K_{binding}$ (M^{-1})	$k_{obs-max}$ (s^{-1})
wild type	190400 ± 1300	3.7 ± 0.01
D383E	338 ± 26	6.5 ± 0.3
D383N	38 ± 4	1.3 ± 0.1
D383A	53 ± 19	0.2 ± 0.06

DISCUSSION

The probable identity of Asp383 as the active site base known to be required for the copper-containing amine oxidase reaction (*19*, *31*) was first reported by Parsons et al. (*13*) in the original crystal structure determination of ECAO. It was subsequently demonstrated by site-directed mutagenesis that this residue is critical to catalytic activity but not to biogenesis of the TPQ cofactor (*20*). Of 14 variants that were studied, only D383E retains any catalytic activity, suggesting the requirement for a carboxylate. The crystal structure of the 2-HP inhibitor complex clearly showed that Asp383 is ideally positioned to abstract a proton from the substrate Schiff base complex (Figure 1, step 1 to 2). This does not, however, rule out the participation of the side chain in other steps of the catalytic cycle, or indeed a structural role, since the mutagenesis results show only that mutants lacking a carboxylate are inactive. Indeed, proton transfers that might involve Asp383, and/or nearby water molecules, also occur in the initial deprotonation of the substrate, substrate Schiff base formation (Figure 1, step 0 to 1), hydrolysis of the product Schiff base (Figure 1, step 3 to 4), and the final displacement of the amine group of aminoquinol to regenerate the TPQ in the oxidative half-cycle (Figure 1, step 4 to 0).

Conservation of the Active Site between Species. The active sites of the four known amine oxidase structures are structurally very similar, as shown in Figure 8. The TPQ exhibits varying degrees of mobility but is clearly flexible in all cases. In the wild type ECAO structure reported here, and in HPAO, the major conformation is as expected for nucleophilic attack by an incoming substrate at C5, with O5 facing the channel to the solvent. In the other two species, the TPQ is reversed, but must be flexible enough to flip readily about χ_2 to generate a productive conformation. Rotation about χ_1 is clearly also possible, as shown by the on-copper coordination of TPQ in the inactivated ECAO (Figure 2) (*13*), one form of AGAO (*15*), and the D383A ECAO mutant (Figures 3 and 5) and the need for this conformation in biogenesis of the cofactor itself (*11*, *15*, *18*). All amine oxidases except PSAO share a similar orientation of the catalytic aspartate, with the plane of the carboxylate group lying approximately perpendicular to the TPQ plane, and contacts from carboxylate oxygens to the TPQ ring carbonyls that are a little longer than would be expected for hydrogen bonds. In PSAO, Asp300 (corresponding to Asp383 of ECAO) lies in the plane of the TPQ and forms a hydrogen bond (2.7 Å) to TPQ O2 (*14*). The aspartate must be protonated to donate a hydrogen bond to a carbonyl oxygen, which is consistent with the acidic pH (4.8) of the PSAO crystals. The other structures were determined at approximately neutral pH (ECAO at pH 7.1, HPAO at pH 6.5, and AGAO at pH 6.8) and do not show strong evidence of hydrogen bonding to TPQ. It should be noted that the pH optimum for k_{cat} per dimer/K_m for ECAO with β-phenylethylamine is 7.0 (*20*), and ECAO crystals are enzymatically active (*13*).

Inspection of the van der Waals surfaces of the TPQ pockets of HPAO, AGAO, and PSAO shows them to have the same wedge shape found in ECAO, and the residues forming the sides of the wedge, Val367 and Asn465, are conserved in all four species. Sequence alignment (*32*) show this conservation extends to other species, except that in mammalian amine oxidases the valine is replaced by alanine. Among amine oxidases from different sources, there is also some conservation of the network of ordered water molecules in the active site (*16*), notably, the axial water coordinated to copper and the water linking this to Oη of a tyrosine (369 in ECAO) that is itself hydrogen bonded to O4 of TPQ. These close similarities suggest that the ECAO mutants provide a good model for the other species.

Orientation and Mobility of TPQ. The three mutant structures demonstrate that the side chain of residue 383 has a profound effect on TPQ mobility and position, as well as on its reactivity. A major role of Asp383 may be to prevent TPQ from migrating to the on-copper conformation found in the inactivated form, since removal of the side chain in

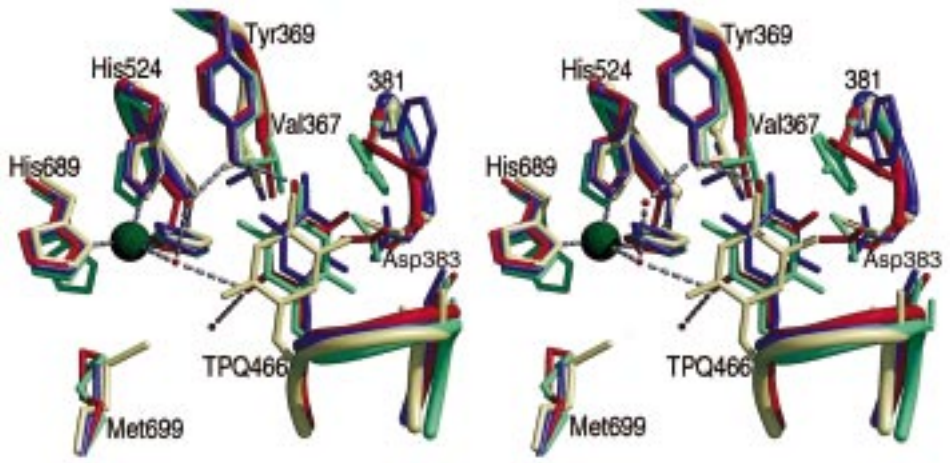

FIGURE 8: Stereoview of the active sites of copper amine oxidases from ECAO (red), AGAO (purple) (*15*), PSAO (green) (*14*), and HPAO (cream) (*16*) from a perspective similar to that shown in Figure 2 in which relevant residues are labeled.

D383A leads to a significant proportion of this orientation. (Figures 3 and 5). Interestingly, this appears not to be due to the loss of clear hydrogen bonding interactions, but rather to a limited number of van der Waals contacts. However, charge may be involved in promoting the off-copper conformation, as a result of either ionization of Asp383 or Glu383 or polarization of the atoms in Asn383. Addition of the single methylene group to the side chain in the D383E mutant has an apparently small effect on the structure, retaining the ability to hold TPQ away from the copper, but dramatically changes TPQ mobility by intruding into the pocket (Figure 4). The refined distance of 3.5 Å between O5 of TPQ and Oϵ2 of Glu383 shows that the reduced mobility is not due to the formation of a hydrogen bond in the variant.

The wedge-shaped pocket for the TPQ, and the freedom of the ring to move within it, is likely to be critical to catalysis. The initial nucleophilic attack of the substrate amine nitrogen on C5 of TPQ must come from above or below the TPQ ring plane, leading to the carbinolamine intermediate. This then dehydrates with the oxygen leaving from the other side of the ring. The intermediate carbinolamine, where both oxygen and substrate nitrogen are bonded simultaneously to tetrahedral C5, would make TPQ wedge-shaped when viewed end-on (i.e., looking from C1 to C4). The wedge shape of the pocket is thus necessary to accommodate this intermediate, and the TPQ must be free to move within it to allow the substrate to attack from one face, presumably that opposite the Asp383 base, and the oxygen to leave from the other. The conservation of the wedge-shaped pocket in other species, with evidence of similar TPQ mobility, is consistent with this interpretation. Taken together, these observations argue for a key role of the active site base in influencing the conformational mobility of the cofactor in addition to its functions in proton transfer.

UV−Vis Spectral Properties of the Wild Type and Variants. The UV−vis absorption spectra of enzyme-bound TPQ and TPQ model compounds have been well characterized (*33*−*37*). Copper-containing amine oxidases in the resting state have a characteristic broad absorption spectrum with a λ_{max} of ∼480 nm at neutral pH, which give them their characteristic pink color. Studies with TPQ model compounds show that protonation at the O4 position causes a shift to shorter wavelengths and a color change from pink to yellow. This may be attributed to protonation of the O4 "phenolate" making the arene ring less electron rich and blue shifting its $\pi \rightarrow \pi^*$ transition. This might explain the observed spectral shifts to shorter wavelengths in the D383N and D383A variants as seen in Figure 6. One might expect that protonation of Asp383 in wild type ECAO would shift the 480 nm peak to shorter wavelengths. However, even at pH 4.2 where Asp383 (p*K* of 6.2) would be protonated, the spectrum is unaltered (data not shown). Also, the p*K* for the phenolate at O4 in TPQ models has been measured (*34*) to be 4.13 and in bovine serum amine oxidase is even lower (3.0) which indicates that at pH 7, virtually all the TPQ would be in the pink O4 phenolate form. At present, we do not have a satisfactory explanation for the visible spectral data though there are parallels to the spectral changes in the photoactive yellow protein observed when Glu46, located adjacent to the 4-hydroxycinnamate chromophore, is mutated to Gln (*38*).

Catalytic Activity of the Variants. Both the D383N and D383A mutants exhibit no measurable enzyme activity, in accordance with the identification of Asp383 as the essential active site base (*20*). The D383E variant is, however, weakly active, but the k_{cat} per dimer is reduced by a factor of 6.4×10^4 compared to that of the wild type, together with a 2-fold increase in the apparent K_m. This change in k_{cat} per dimer is much greater than would be expected from the kinetic constants for 2-HP binding which models step 1 in Figure 1, but the overall catalytic process has several other steps where the base is involved and where TPQ mobility might be important. Kinetic isotope effects of benzylamine oxidation by PPAO, BSAO, and HPAO demonstrated that the C−H bond cleavage step catalyzed by the aspartate residue is fully rate-determining during the reductive half-reaction (*7*, *31*, *39*). Although the carboxylate group of Glu383 lies in a position similar to that of Asp383, it points in a slightly different direction and the extra steric crowding may further distort the geometry away from an optimal arrangement for hydrogen abstraction. In the oxidative half-cycle, the displacement of the amino group from the iminoquinone probably involves nucleophilic attack of a water molecule at C5, leading again to a wedge-shaped intermediate whose formation could be impeded by intrusion of Glu383.

Binding of 2-Hydrazinopyridine (2-HP) to the Variants. Phenylhydrazine derivatives act as suicide inhibitors of copper amine oxidases and have been used for quantitative titration of the average number of reactive TPQ moieties present in the enzyme (*40*). These inhibitors form a Schiff base with TPQ C5 as for normal substrates, but the abstraction of the proton by the active site base (Figure 1, step 1 to 2) becomes very unfavorable, trapping the reaction at step 1. The inhibitor 2-HP was used by Wilmot et al. (*20*) to generate a stable complex for crystal structure determination. The study of the kinetics of association of 2-HP with the wild type and variant proteins gives an apparent binding constant for the initial complex between 2-HP and the enzyme. Caution is needed in the interpretation of data since there is no direct evidence that it relates to a true equilibrium between the enzyme and the inhibitor. For the wild type, the apparent $K_{binding}$ is strong (190 400 M^{-1}) but decreases ~500-fold in D383E to 346 M^{-1}, and then by a further factor of ~10-fold in D383N and D383A.

The D383N variant is isostructural to wild type, with apparently similar TPQ mobility although the very large decrease in the apparent 2-HP binding constant (by ~10^3) demonstrates a requirement for a carboxylate rather than for an amide group.

For D383E, which like the wild type enzyme has a carboxylate, the 500-fold decrease in the apparent binding constant for 2-HP relative to wild type may be due to the decreased mobility of the TPQ. This would hinder nucleophilic attack on C5 by 2-HP from the face opposite Glu383 as the inhibitor would require access to the face of the TPQ which is packed against Asn465.

It is not easy to draw conclusions from the values of $k_{obs-max}$ other than to say that the rate-limiting step for 2-HP complex formation depends on the residue at position 383. Caution is needed in drawing comparisons between the $k_{obs-max}$ for 2-HP complex formation and the k_{cat} for substrate turnover since the rate-limiting steps are almost certainly different.

Concluding Remarks. The base, Asp383 in ECAO, is not only critical in several proton transfer steps in the reaction cycle but also plays a key role in controlling both the conformation and flexibility of the TPQ cofactor. Replacement of Asp383 with the isostructural, but chemically different, Asn383 does not affect the TPQ conformation or dynamics appreciably, but abolishes catalytic activity by removing the base. Removal of the side chain, as in Ala383, additionally allows TPQ greater conformational freedom to migrate to the copper. The greatly reduced activity of Glu383 appears to result from its protrusion into the wedge-shaped pocket, which has evolved to allow TPQ to move and facilitate access to the face of the ring at C5 and accommodate the ensuing tetrahedral intermediate(s).

ACKNOWLEDGMENT

We thank Alison Ashcroft for many helpful discussions on mass spectrometry and acknowledge Dr. Fadi R. Abou-Shakra of Micromass UK Ltd. for analyzing samples and for technical discussions. We thank Judith Klinman for helpful comments on the manuscript and the staff at the Daresbury SRS and at ESRF Grenoble for help with data collection.

NOTE ADDED IN PROOF

The preceding paper by Plastino et al. (*41*) describes an independent study in which active site mutations of the catalytic base D319 of the *H. polymorpha* copper amine oxidase were investigated. The enzymes from *H. polymorpha* and *E. coli* exhibit overall structural and mechanistic similarities. However, subtle active site differences must exist between the two enzymes that lead similar amino acid substitutions to confer rather distinct properties.

REFERENCES

1. Hartmann, C., and Klinman, J. P. (1991) *Biochemistry 30*, 4605−4611.
2. Mu, D., and Klinman, J. P. (1995) *Methods Enzymol. 258*, 114−122.
3. McIntire, W. S. (1998) *Annu. Rev. Nutr. 18*, 145−177.
4. Møller, S. G., and McPherson, M. J. (1998) *Plant J. 13*, 781−791.
5. Bono, P., Salmi, M., Smith, D. J., and Jalkanen, S. (1998) *J. Immunol. 160*, 5563−5571.
6. Boomsma, F., vanVeldhuisen, D. J., deKam, P. J., ManintVeld, A. J., Mosterd, A., Lie, K. I., and Schalekamp, M. (1997) *Cardiovasc. Res. 33*, 387−391.
7. Klinman, J. P., and Mu, D. (1994) *Annu. Rev. Biochem. 63*, 299−344.
8. Knowles, P. F., and Dooley, D. M. (1994) in *Metal Ions in Biological Systems* (Sigel, H., and Sigel, A., Eds.) Vol. 30, pp 361−403, Marcel Dekker, New York.
9. Janes, S. M., Palcic, M. M., Scaman, C. H., Smith, A. J., Brown, D. E., Dooley, D. M., Mure, M., and Klinman, J. P. (1992) *Biochemistry 31*, 12147−12154.
10. Matsuzaki, R., Fukui, T., Sato, H., Ozaki, Y., and Tanizawa, K. (1994) *FEBS Lett. 351*, 360−364.
11. Cai, D. Y., and Klinman, J. P. (1994) *J. Biol. Chem. 269*, 32039−32042.
12. Ruggiero, C. E., Smith, J. A., Tanizawa, K., and Dooley, D. M. (1997) *Biochemistry 36*, 1953−1959.
13. Parsons, M. R., Convery, M. A., Wilmot, C. M., Yadav, K. D. S., Blakeley, V., Corner, A. S., Phillips, S. E. V., McPherson, M. J., and Knowles, P. F. (1995) *Structure 3*, 1171−1184.
14. Kumar, V., Dooley, D. M., Freeman, H. C., Guss, J. M., Harvey, I., McGuirl, M. A., Wilce, M. C. J., and Zubak, V. M. (1996) *Structure 4*, 943−955.
15. Wilce, M. C. J., Dooley, D. M., Freeman, H. C., Guss, J. M., Matsunami, H., McIntire, W. S., Ruggiero, C. E., Tanizawa, K., and Yamaguchi, H. (1997) *Biochemistry 36*, 16116−16133.
16. Li, R. B., Klinman, J. P., and Mathews, F. S. (1998) *Structure 6*, 293−307.
17. Mu, D., Janes, S. M., Smith, A. J., Brown, D. E., Dooley, D. M., and Klinman, J. P. (1992) *J. Biol. Chem. 267*, 7979−7982.
18. Tanizawa, K. (1995) *J. Biochem. 118*, 671−678.
19. Farnum, M., Palcic, M., and Klinman, J. P. (1986) *Biochemistry 25*, 1898−1904.
20. Wilmot, C. M., Murray, J. M., Alton, G., Parsons, M. R., Convery, M. A., Blakeley, V., Corner, A. S., Palcic, M. M., Knowles, P. F., McPherson, M. J., and Phillips, S. E. V. (1997) *Biochemistry 36*, 1608−1620.
21. Sarkar, G., and Sommer, S. S. (1990) *BioTechniques 8*, 404−407.
22. Sambrook, J., Fritsch, E. F., and Maniatis, T. (1989) *Molecular Cloning*, 2nd ed., Cold Spring Harbor Laboratory Press, Cold Spring Harbor, NY.
23. Leslie, A. G. W. (1992) *Joint CCP4 and ESF-EACBM Newsletter on Protein Crystallography*, Vol. 26, Daresbury Laboratory, Warrington, U.K.
24. Collaborative Computational Project Number 4 (1994) *Acta Crystallogr. D50*, 760−763.
25. Brünger, A. T., Adams, P. D., Clore, G. M., DeLano, W. L., Gros, P., GrosseKunstleve, R. W., Jiang, J. S., Kuszewski, J.,

Nilges, M., Pannu, N. S., Read, R. J., Rice, L. M., Simonson, T., and Warren, G. L. (1998) *Acta Crystallogr. D54*, 905−921.
26. Read, R. J. (1986) *Acta Crystallogr. A42*, 140−149.
27. Jones, T. A., Zou, J. Y., Cowan, S. W., and Kjeldgaard, M. (1991) *Acta Crystallogr. A*47, 110−119.
28. Pannu, N. S., and Read, R. J. (1996) *Acta Crystallogr. A52*, 659−668.
29. Saysell, C. G., Murray, J. M., Wilmot, C. M., Brown, D. E., Dooley, D. M., Phillips, S. E. V., McPherson, M. J., and Knowles, P. F. (1999) *J. Mol. Catal. B: Enzym.* (in press).
30. Laskowski, R. A., Macarthur, M. W., Moss, D. S., and Thornton, J. M. (1993) *J. Appl. Crystallogr. 26*, 283−291.
31. Olsson, B., Olsson, J., and Pettersson, G. (1976) *Eur. J. Biochem. 64*, 327−331.
32. Tipping, A. J., and McPherson, M. J. (1995) *J. Biol. Chem. 270*, 16939−16946.
33. Hartmann, C., Brzovic, P., and Klinman, J. P. (1993) *Biochemistry 32*, 2234−2241.
34. Mure, M., and Klinman, J. P. (1993) *J. Am. Chem. Soc. 115*, 7117−7127.
35. Turowski, P. N., McGuirl, M. A., and Dooley, D. M. (1993) *J. Biol. Chem. 268*, 17680−17682.
36. Mure, M., and Klinman, J. P. (1995) *J. Am. Chem. Soc. 117*, 8707−8718.
37. Mure, M., and Klinman, J. P. (1995) *J. Am. Chem. Soc. 117*, 8698−8706.
38. Xie, A. H., Hoff, W. D., Kroon, A. R., and Hellingwerf, K. J. (1996) *Biochemistry 35*, 14671−14678.
39. Cai, D. Y., and Klinman, J. P. (1994) *Biochemistry 33*, 7647−7653.
40. Janes, S. M., and Klinman, J. P. (1995) *Methods Enzymol. 258*, 20−34.
41. Plastino, J., Green, E. L., Sanders-Loehr, J., and Klinman, J. P. (1999) *Biochemistry 38*, 8204−8216.

BI9900469